Tril dampens Nodal signaling through Pellino2- and Traf6-mediated activation of Nedd4l

Hyung-Seok Kim[a,1], Yangsook Song Green[a,1,2], Yuanyuan Xie[a,3], and Jan L. Christian[a,b,4]

[a]Department of Neurobiology, University of Utah, Salt Lake City, UT 84112; and [b]Department of Internal Medicine, Division of Hematology and Hematologic Malignancies, School of Medicine, University of Utah, Salt Lake City, UT 84112

Toll-like receptor 4 (Tlr) interactor with leucine-rich repeats (Tril) functions as a Tlr coreceptor to mediate innate immunity in adults. In *Xenopus* embryos, Tril triggers degradation of the transforming growth factor β (Tgf-ß) family inhibitor, Smad7. This enhances bone morphogenetic protein (Bmp) signaling to enable ventral mesoderm to commit to a blood fate. Here, we show that Tril simultaneously dampens Nodal signaling by catalytically activating the ubiquitin ligase NEDD4 Like (Nedd4l). Nedd4l then targets Nodal receptors for degradation. How Tril signals are transduced in a nonimmune context is unknown. We identify the ubiquitin ligase Pellino2 as a protein that binds to the cytoplasmic tail of Tril and subsequently forms a complex with Nedd4l and another E3 ligase, TNF-receptor associated factor 6 (Traf6). Pellino2 and Traf6 are essential for catalytic activation of Nedd4l, both in *Xenopus* and in mammalian cells. Traf6 ubiquitinates Nedd4l, which is then recruited to membrane compartments where activation occurs. Collectively, our findings reveal that Tril initiates a noncanonical Tlr-like signaling cascade to activate Nedd4l, thereby coordinately regulating the Bmp and Nodal arms of the Tgf-ß superfamily during vertebrate development.

Tril | Nodal | Nedd4l | Pellino | *Xenopus*

The two arms of the transforming growth factor β (Tgf-ß) superfamily, which are activated by Tgf-ß/Nodal or bone morphogenetic protein (Bmp) ligands, respectively, often operate simultaneously to achieve differing goals. During development, Nodal signaling induces mesendoderm and is required for gastrulation and anterior patterning, while Bmps operate at the same time to specify ventral and posterior fate (1, 2). In cancer stem cells, Bmp signaling inhibits self-renewal and thus acts as a barrier to tumor progression and metastasis, whereas Nodal signaling positively regulates cancer stem cell proliferation (3). A proper balance of Bmp and Tgf-ß/Nodal signaling is critical to ensure normal development and to prevent disease, and yet our knowledge of how these pathways are coordinately regulated is incomplete.

Bmps and Nodals activate transmembrane serine/threonine kinase receptors that phosphorylate pathway-specific Smads (Smad1/5/8 for Bmps, Smad2 for Nodal). Phosphorylated Smads (pSmads) then recruit the co-Smad, Smad4, and translocate to the nucleus to induce target gene expression. Smad7 is a target gene induced by both pSmad2 and pSmad1/5/8 and is a central hub for negative feedback regulation of Nodal and Bmp signaling (4). Smad7 recruits E3 ubiquitin ligases to activated Nodal and Bmp receptors, targeting them for degradation, and can also block transcriptional responses downstream of pSmads (4).

We identified *tril* (*tlr4 interactor with leucine-rich repeats*) as a gene that is coexpressed with *bmps* in ectoderm and ventral mesoderm during *Xenopus* gastrulation (5). Tril is a transmembrane protein that functions as a coreceptor for Toll-like Receptor 3 (TLR3) and TLR4 to mediate innate immune responses in the brain of adult mammals (6–8). We showed that Tril triggers degradation of Smad7 protein during gastrulation, thereby relieving repression of Bmp signaling to enable ventral mesoderm

to be specified as blood. How Tril signals are transduced in a nonimmune setting remains unknown.

In *Xenopus, nodal* family genes are coexpressed with *tril* throughout the mesoderm during gastrulation (9–12). Because Smad7 is a potent inhibitor of Tgf-ß/Nodal signaling, it seemed likely that Tril-mediated degradation of Smad7 functions to enhance Nodal signaling in early embryos, similar to its role in augmenting Bmp signals. Surprisingly, we found that Tril instead dampens Nodal signaling and that it does so through a mechanism independent of Smad7 degradation. Furthermore, we found that Tril signals are transduced using components of Tlr signaling cascades that operate in the immune system. Our findings uncover essential nonimmune functions for Tril in coordinately regulating Bmp and Nodal signaling during early vertebrate development.

Results

Tril Dampens Nodal Signals. At the onset of gastrulation, Nodal signaling is highest in dorsal cells (13) and induces a signaling center, the Spemann organizer, that is required for gastrulation and neural induction (2). *tril* is expressed in ventral ectoderm (5) and in dorsal mesodermal cells (Fig. 1*A*) at the onset of gastrulation, and expression spreads to include ventral mesoderm shortly thereafter (5). This raises the possibility that Tril-mediated degradation of Smad7 is required to augment Nodal signaling (Fig. 1 *B, Top*). If so, then loss of Tril should lead to reduced Nodal output (Fig. 1 *B, Bottom*). To test this, we injected previously validated translation blocking Tril antisense morpholino oligonucleotides (MOs) (5) into dorsal cells of four-cell embryos. Embryos

Significance

A proper balance of Bmp and Tgf-ß/Nodal signaling is critical to ensure normal development and to prevent disease. Our studies identify a signaling cascade that functions to coordinately enhance Bmp signaling and reduce Nodal output by activating the ubiquitin ligase Nedd4l. Mutations in *NEDD4L* that lead to gain or loss of activity underlie congenital disorders and disease in humans. Understanding how Nedd4l activity is regulated in different contexts may provide insight into how mutations in *NEDD4L* result in human pathology.
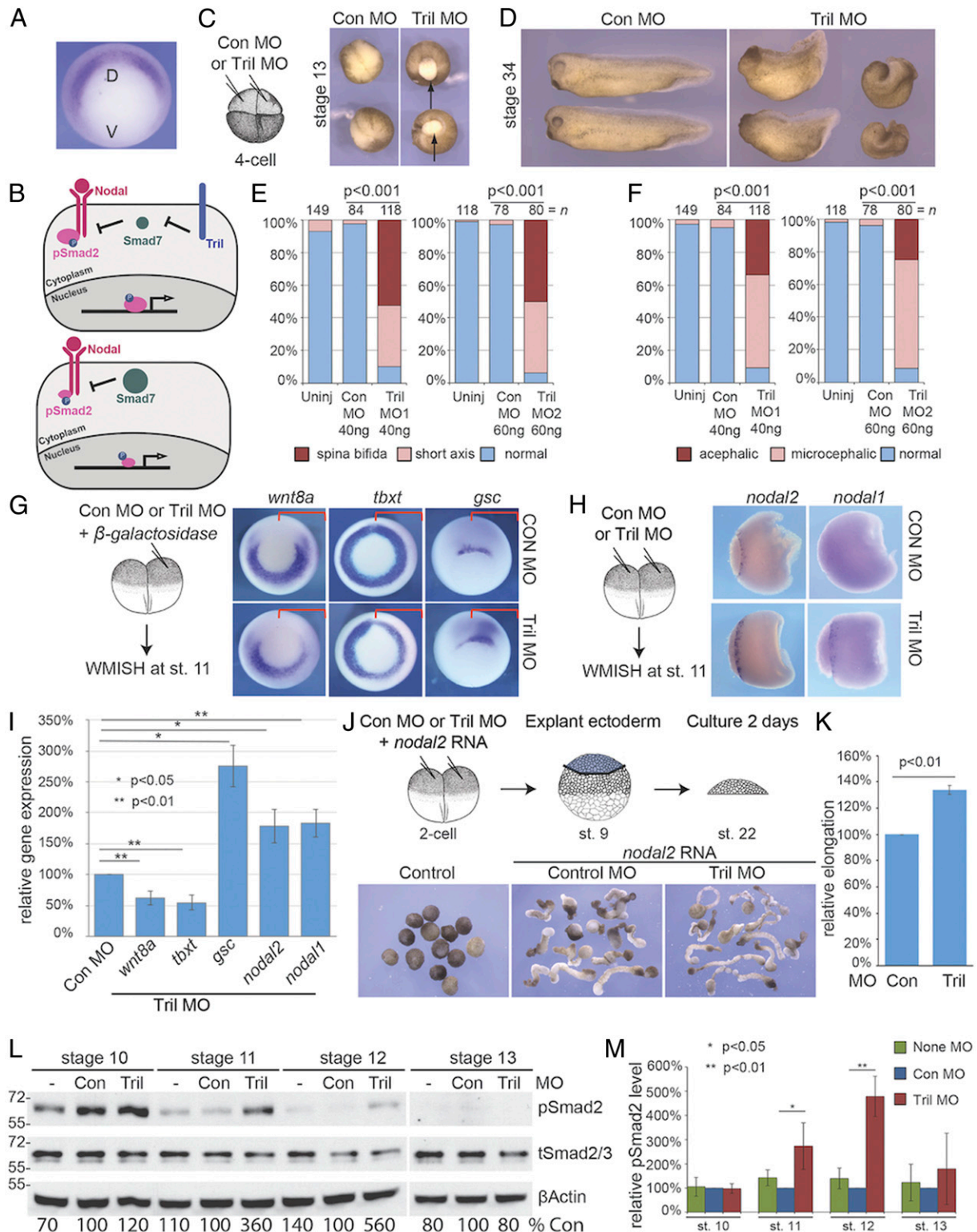
Fig. 1. Tril dampens Nodal signals. (*A*) Whole mount in situ hybridization (WMISH) analysis of *tril* at st. 10. Vegetal view. D; dorsal, V; ventral. (*B*) Predicted Tril function in degrading Smad7 to relieve Nodal inhibition (*Top*). If correct, loss of Tril would lead to reduced Nodal signals (*Bottom*). (*C–F*) Control (Con) or Tril MOs (20 ng) were injected into dorsal cells and representative embryos photographed at st. 13 (arrows denote open blastopore) (*C*) or st. 34 (*D*). Defects were quantified in embryos pooled from five biological replicates (*E* and *F*). (*G*) *β-galactosidase* RNA was coinjected with Tril or Con MOs as illustrated. Embryos were stained for β-Galactosidase at st. 11 to identify cells that received the MOs (red bracket) followed by WMISH. (*H* and *I*) Tril or Con MOs were injected into both cells of two-cell embryos. Expression of Nodal target genes was analyzed by WMISH (*H*) or qPCR (*I*). (*J* and *K*) Tril or Con MOs were injected into two-cell embryos with or without *nodal2* RNA (5 pg). Ectoderm was explanted and cultured until sibling embryos reached stage 22. (*L* and *M*) Tril, Con, or no (-) MOs were injected into both cells of two-cell embryos. Levels of pSmad2, total Smad2 (tSmad2), and β-Actin were analyzed by immunoblot. A representative blot (*L*) and normalized data (levels of pSmad2 normalized to β-Actin from four biological replicates) (*M*) are shown.

injected with either of two Tril MOs (MO1 or MO2) showed delayed and abnormal gastrulation relative to controls, as indicated by an open blastopore (Fig. 1C, arrows). At the tailbud stage, Tril morphants had a shortened anterior–posterior axis and/or spina bifida (Fig. 1 D and E) and were microcephalic or acephalic (Fig. 1 D and F). Expression of the forebrain marker *eomes* was absent or reduced in Tril morphants, whereas expression of the spinal cord marker, *hoxa9*, was reduced in a subset of the most severely impaired Tril morphants (*SI Appendix*, Fig. S1A) but was never absent. Thus Tril, like Nodal, is required for normal gastrulation and head development.

Tril is a transmembrane protein with a large extracellular domain (ECD) that contains leucine-rich repeats, a fibronectin type III (FN) domain, and a small intracellular domain (ICD) (*SI Appendix*, Fig. S1B). A Tril deletion mutant lacking the FN domain (TrilΔFN) functions as a dominant mutant, while a mutant lacking the ICD (TrilΔICD) neither activates nor inactivates Tril signaling (14). When RNA encoding TrilΔFN was injected into dorsal blastomeres of four-cell embryos, gastrulation was defective, embryos showed spina bifida or a shortened axis, and the head was reduced or absent at the tailbud stage (*SI Appendix*, Fig. S1 B–D). By contrast, embryos injected with *trilΔICD* RNA developed normally (*SI Appendix*, Fig. S1 B–D). Thus, the defects in Tril morphants can be phenocopied by ectopic expression of a dominant mutant form of Tril.

We next analyzed expression of Nodal target genes. MOs were injected into one cell of two-cell embryos, together with RNA encoding β-Galactosidase. Embryos were stained for β-Galactosidase activity at stage (st.) 11, followed by analysis of gene expression by whole mount in situ hybridization. Expression of *wnt8a* and *tbxt* was reduced (Fig. 1G, red bar marks injected side identified by Red-Gal staining, although staining is not visible in vegetal views), and this reduction was partially rescued by injection of *tril* RNA (*SI Appendix*, Fig. S1 E–G). By contrast, expression of *gsc* was elevated in cells receiving the Tril MO (Fig. 1G). Expression of the direct target genes *nodal1* and *nodal2* was elevated throughout their expression domain when Tril MOs were delivered to both cells of two-cell embryos (Fig. 1H). qPCR analysis confirmed that expression of *wnt8a* and *tbxt* was significantly reduced, while expression of *gsc*, *nodal1*, and *nodal2* was increased in Tril morphants (Fig. 1I). Elevated Nodal signaling leads to enhanced expression of *gsc*, which then represses expression of *wnt8a* (15) and *tbxt* (16), leading to defects in gastrulation and head development (17). These results suggest that Tril is required to dampen rather than enhance Nodal signaling.

We then compared the ability of Nodal to induce elongation of ectodermal explants in the presence and absence of Tril. MOs were coinjected with *nodal2* RNA (5 picograms [pg]); ectoderm was explanted at st. 9 and cultured until sibling embryos reached stage 22. Nodal induced a more robust elongation of ectoderm isolated from Tril morphants than that isolated from controls (Fig. 1 J and K), again suggesting that Tril dampens Nodal responsiveness.

We used immunoblots to compare levels of pSmad2 in Tril and control morphant embryos. Relative levels of pSmad2 were significantly elevated in Tril morphants during midgastrulation (st. 11 and 12) before returning to control levels at the end of gastrulation (st. 13) (Fig. 1 L and M). Injection of RNA encoding Tril into both dorsal blastomeres of four-cell embryos partially rescued the elevated pSmad2 in Tril morphants (*SI Appendix*, Fig. S1H), and pSmad2 levels were also elevated in wild-type embryos expressing the dominant mutant form TrilΔFN (*SI Appendix*, Fig. S1I), confirming that Tril is required to dampen Nodal signaling.

Tril Dampens Nodal Pathway Activation at the Level of pSmad2 Phosphorylation. The observation that Nodal signaling is enhanced in Tril morphants was unexpected given our previous finding that levels of Smad7, a potent Nodal inhibitor, are elevated

in these embryos (5, 14). This leaves open the possibility that Tril triggers degradation of Smad7 only in ventral cells, where BMP signaling is active and not in dorsal cells, where Nodal signaling initiates. Contrary to this possibility, we found that levels of Smad7 protein are significantly elevated in dorsal cells of Tril morphants, as analyzed by immunostaining of ectopic Smad7myc (Fig. 2A). Immunoblot analysis confirmed that Smad7myc protein levels are elevated in both dorsal (Fig. 2B and *SI Appendix*, Fig. S2A) and ventral cells of Tril morphants (*SI Appendix*, Fig. S2A). Thus, Tril dampens Nodal signaling during gastrulation despite its ability to promote degradation of the Nodal inhibitor, Smad7 (Fig. 2C).

To ask where in the Nodal signaling cascade Tril functions, we activated Nodal signaling in ectodermal explants isolated from control or Tril morphants at the level of the ligand, activated receptor, or activated pSmad2 and compared transcriptional outputs. MOs were injected together with relevant RNAs into both cells of two-cell embryos, ectoderm was explanted at st. 9, and harvested for analysis of *nodal1* and *nodal2* by qPCR at st.11 (Fig. 2D). When pSmad2-dependent signaling was activated at the level of ligand, by incubating explants in media containing activin, or at the level of the receptor, by injection of RNA encoding a constitutively active Nodal receptor (ca-ALK4) (18), expression of *nodal1* and *nodal2* was elevated in Tril morphant relative to control ectoderm (Fig. 2 E, F, H, and I). By contrast, when the Nodal pathway was activated by injection of RNA encoding constitutively active, phosphomimetic Smad2 (ca-Smad2), levels of *nodal1* and *nodal2* transcripts were reduced in Tril morphant ectoderm relative to controls (Fig. 2 G and J). These data show that Tril acts downstream of activated Nodal receptors but upstream of pSmad2-mediated transcription of target genes to dampen Nodal responses. When the Nodal pathway is activated by ca-Smad2, the elevated levels of Smad7 in Tril morphants (Fig. 2B) may act in the nucleus to negatively regulate target gene activation (4).

To test whether Tril dampens Nodal signaling at the level of pathway activation, for example by inducing receptor degradation, and/or whether it functions to terminate Nodal signaling, for example by inducing degradation of pSmad2, we compared the timing of Smad2 phosphorylation and decay in ectodermal explants isolated from control or Tril morphants. Explants were isolated at stage 10, incubated in media containing activin for 30 min, washed, and then transferred to media containing SB431542 to block further receptor kinase activity. pSmad2 levels were higher in Tril morphant ectoderm in controls following 30 min of activin stimulation (Fig. 2K) but dropped rapidly and with similar kinetics in control and Tril morphant explants following receptor inactivation (Fig. 2 K and L). The same rapid decay of endogenous pSmad2 levels was observed in control and Tril morphants following incubation of whole embryos in SB431542 (*SI Appendix*, Fig. S2 B and C). Thus, Tril dampens Nodal signaling at the level of receptor-mediated phosphorylation of pSmad2 (Fig. 2M).

Nedd4l Dampens Nodal Signaling at the Level of Smad2 Phosphorylation. One way that Tril might dampen Nodal signaling is by positively regulating NEDD4 Like (Nedd4l) E3 Ubiquitin Ligase, which targets activated Tgf-ß–family receptors for degradation (19). We first tested whether endogenous Nedd4l is required to dampen Nodal signaling during gastrulation. A previously validated translation blocking Nedd4l antisense MO (20) reduced endogenous Nedd4l protein levels by 60% (Fig. 3A). Depletion of Nedd4l in dorsal cells phenocopied the defects in gastrulation, axial extension, and head development (Fig. 3 B–D) that are observed in Tril morphants. Expression of *tbxt* was absent ($n = 4/23$) or reduced (Fig. 3 E, E', $n = 19/23$) in st. 11 Nedd4l morphants, consistent with previous reports (20), whereas expression of *gsc* (Fig. 3 F, F', $n = 29/29$) and *nodal2* (Fig. 3 G, G', 26/29) were enhanced. Furthermore, levels of pSmad2 were elevated in Nedd4l morphants throughout gastrulation (Fig. 3 I and J), and this was rescued by
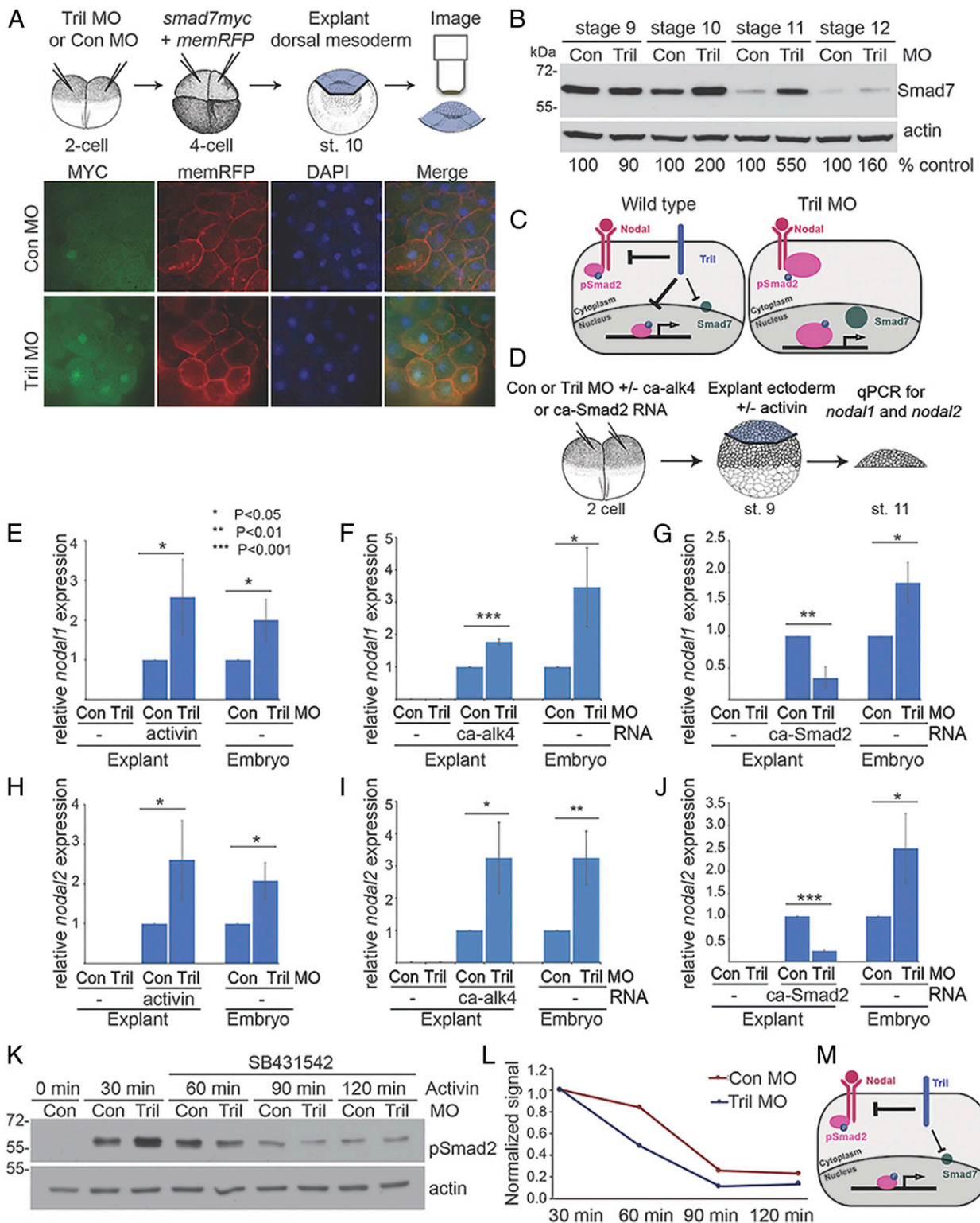
Kim et al.
Tril dampens Nodal signaling through Pellino2- and Traf6-mediated activation of Nedd4l

PNAS | 3 of 12
https://doi.org/10.1073/pnas.2104661118

Fig. 2. Tril dampens Nodal pathway activation at the level of Smad2 phosphorylation. (*A* and *B*) RNA encoding Smad7myc (50 pg) was injected into dorsal cells of four-cell embryos. The dorsal quadrant was explanted from st. 10 Tril or control (Con) morphants and immunostained for myc and RFP (*A*), or whole embryos were subjected to immmunoblot analysis at st. 11 (*B*). Smad7 levels in Tril morphants relative to Cons are reported below each lane. (*C*) Tril inhibits Nodal signaling independent of its ability to trigger degradation of Smad7 (*Left*). In Tril morphants, Nodal signaling is elevated despite high levels of Smad7 (*Right*). (*D–J*) Tril or Con MOs were injected $^{+/-}$ RNA encoding caALK (500 pg) or caSmad2 (25 pg). Ectoderm was explanted at st. 9, cultured in the presence or absence of activin (3 ng/mL) until st. 11, and gene expression analyzed by qPCR as illustrated. Levels of *nodal1* or *nodal2* are reported as a percentage of Con levels. (*K* and *L*) Immunoblot showing the decay of pSmad2 in ectodermal explants isolated from Con or Tril morphants, treated with Activin (20 ng/mL) for 30 min, and then chased in the presence of SB431542 (50 μM). A representative immmunoblot (*K*) and relative pSmad2 levels in Tril and Con morphants at 30 min, followed by the decay of pSmad2 signal over time (*L*) are shown. (*M*) Tril inhibits Nodal signaling at the level of receptor-mediated phosphorylation of pSmad2.
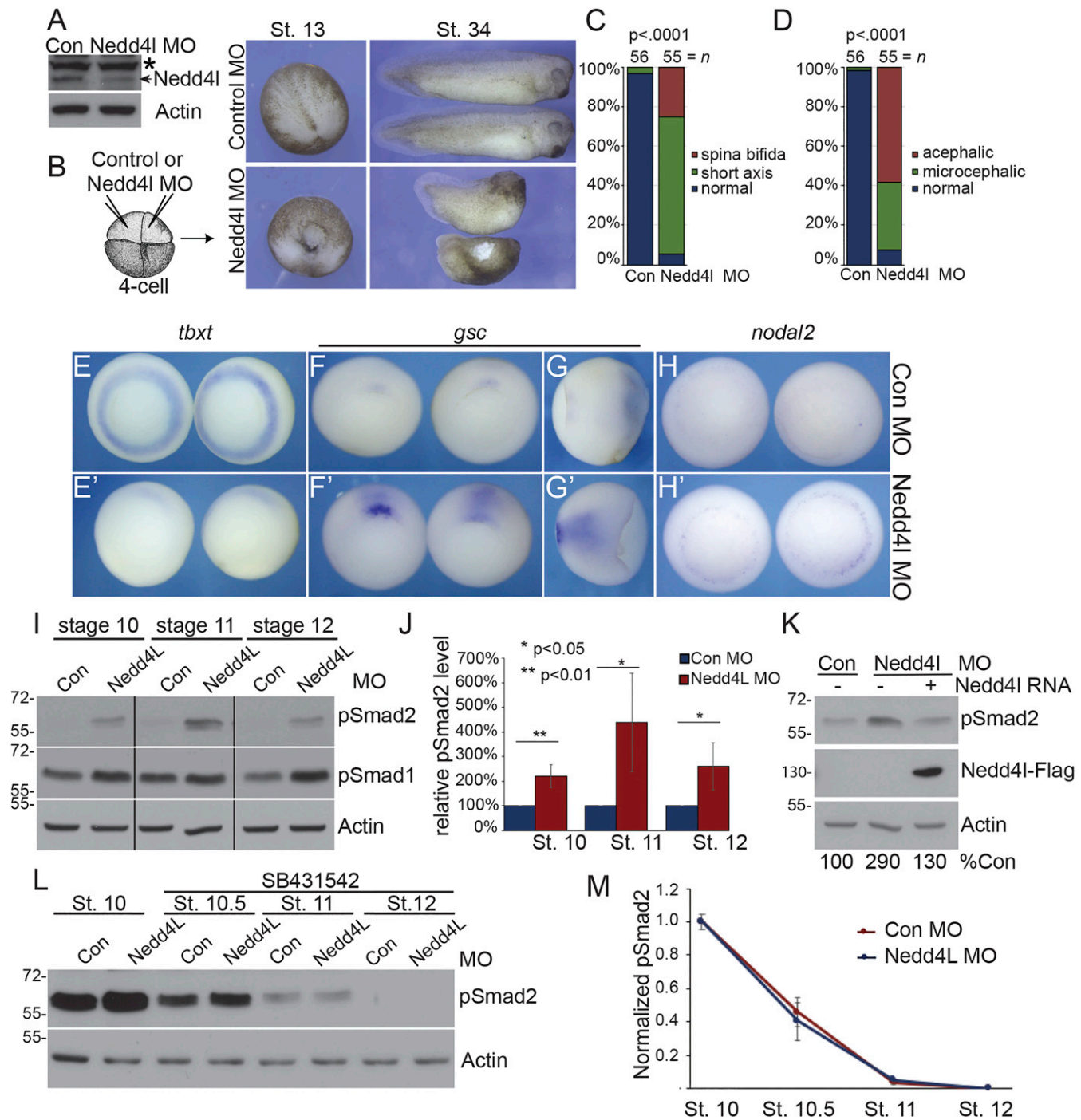
Fig. 3. Nedd4l dampens Nodal signaling at the level of Smad2 phosphorylation. (*A*) Immunoblot analysis of endogenous Nedd4l levels in st. 11 control (Con) and Nedd4l MO (30 ng) injected embryos. Arrow, specific signal; asterisk, nonspecific band. (*B–D*) MOs were targeted to dorsal cells of four-cell embryos. Representative embryos were photographed (*B*), and defects were quantified in embryos pooled from three replicates (*C* and *D*). (*E–H'*) Expression of Nodal target genes in Nedd4l and Con morphant embryos at st. 11. Vegetal views are shown except for *G* and *G'*, which are dorsal views. (*I* and *J*) Immunoblot analysis of pSmad2 and pSmad1 levels in Con and Nedd4l morphants. A representative immunoblot (*I*) and normalized levels of pSmad2 (*J*) are shown. All lanes are from the same pSmad immunoblot, aligned following removal of intervening lanes (marked by black bars). (*K*) Immunoblot analysis of pSmad2 levels in st. 11 embryos expressing Con or Nedd4l MOs alone or together with Nedd4l RNA (100 pg) in dorsal cells. (*L* and *M*) Con or Tril morphants were cultured in the presence of SB431542 (100 μM) to terminate endogenous receptor activity. Levels of pSmad2 were analyzed by immunoblot. A representative Western blot (*L*) and normalized pSmad2 levels in Tril and Con morphants at st. 10, followed by the decay of pSmad2 signal over time (*M*) are shown.

injection of RNA encoding Nedd4l into both dorsal blastomeres of four-cell embryos (Fig. 3*K*). By contrast, although there was a slight increase in pSmad1levels in Tril morphants at st. 12 in the experiment shown, depletion of Nedd4l did not reproducibly affect pSmad1 levels in other replicates (Fig. 3*I*). Thus, Nedd4l is required to dampen Nodal but not BMP signaling.

In addition to targeting Nodal receptors for degradation, Nedd4l can terminate Nodal signaling by promoting degradation

Kim et al.
Tril dampens Nodal signaling through Pellino2- and Traf6-mediated activation of Nedd4l

PNAS | 5 of 12
https://doi.org/10.1073/pnas.2104661118

of pSmad2 (21). To ask whether this occurs during *Xenopus* gastrulation, we compared the timing of pSmad2 decay in response to endogenous nodal signals. One-cell embryos were injected with control or Nedd4l MOs, incubated in SB431542 beginning at stage 10 and harvested for immunoblot analysis of pSmad2 levels at stage 10 to 12. When Smad2 phosphorylation was blocked by incubation in SB431542, pSmad2 levels dropped rapidly and with similar kinetics in control and Nedd4l morphant embryos (Fig. 3 *L* and *M*). These results suggest that, in the context of *Xenopus* mesoderm induction, Nedd4l does not strongly enhance pSmad2 degradation.

Tril Triggers the Ubiquitin Ligase Activity of Nedd4l. We next asked whether Tril positively regulates Nedd4l stability and/or activity. In Tril morphants, levels of endogenous Nedd4l protein were reduced to less than 50% of control levels at st. 11 (Fig. 4 *A* and *B*). Similarly, steady-state levels of ectopic, overexpressed Nedd4lFlag protein were reduced by 20 to 40% in Tril morphants relative to controls and were rescued by coinjection of *tril* RNA (*SI Appendix*, Fig. S3*A*). In control embryos, ectopic expression of Trill increased steady-state levels of Nedd4lFlag (*SI Appendix*, Fig. S3*B*). Thus, Tril is necessary and sufficient to maintain or enhance Nedd4l protein levels.

Following enzymatic activation, Nedd4l autocatalytically ubiquitinates itself leading to tightly coupled degradation of Nedd4l and its substrate (22). We asked whether the catalytic activity of Nedd4l is required for accelerated turnover in Tril morphants by comparing steady-state levels of Nedd4l or a catalytically inactive form of Nedd4l (Nedd4l^{C938A}) in control or Tril morphants at st. 11. Levels of Nedd4l^{C938A} were higher than levels of wild-type Nedd4l, consistent with a function for autocatalytic Nedd4l degradation in vivo (Fig. 4*C*). Levels of both Nedd4l and Nedd4l^{C938A} were reduced in Tril morphants relative to controls (Fig. 4 *C* and *D*). Thus, the reduction in Nedd4l levels in Tril morphants occurs independent of self-degradation.

If Tril dampens Nodal activity solely by raising Nedd4l protein levels, then it should be possible to rescue the elevated pSmad2 in Tril morphants by ectopically expressing Nedd4l. To test this, Tril MOs were targeted to dorsal blastomeres of four-cell embryos either alone or together with RNA encoding Nedd4l. Overexpression of Nedd4l was not sufficient to enhance degradation of pSmad2 in controls or to rescue high pSmad2 levels in morphants (Fig. 4 *E* and *F*). We then repeated this experiment with a constitutively active form of Nedd4l (Nedd4l^{R893Q}) (23). Overexpression of Nedd4l^{R893Q} reduced steady-state levels of pSmad2 in controls and rescued elevated pSmad2 levels in Tril morphants
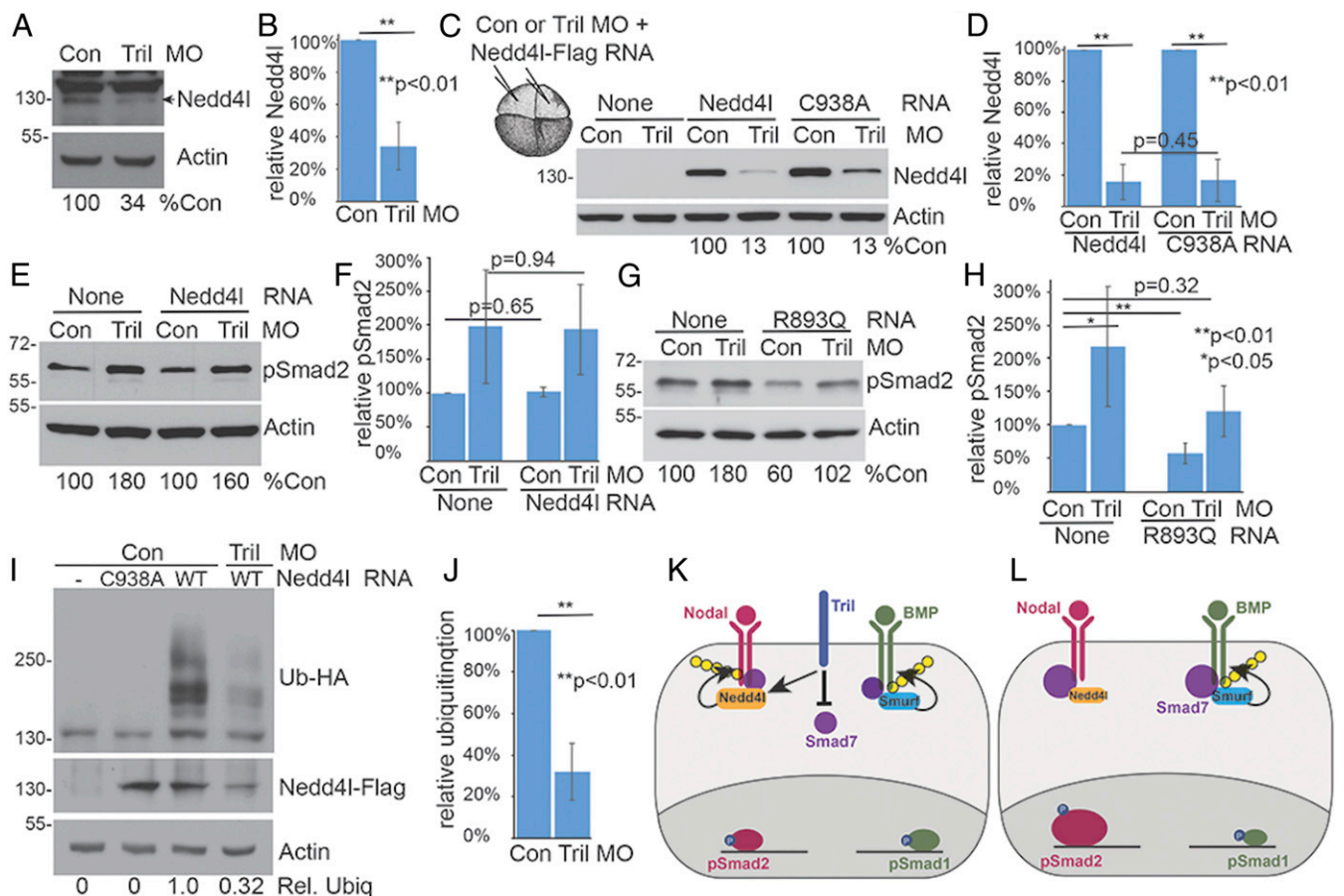

Fig. 4. Tril triggers the ubiquitin ligase activity of Nedd4l. (*A* and *B*) Immunoblot analysis of endogenous Nedd4l levels (arrow) in st. 11 control (Con) and Tril morphant (40 ng) embryos. (*C* and *D*) Immunoblot analysis of Nedd4lFlag levels in Con or Tril morphants (st. 11) expressing Nedd4lFlag or Nedd4lFlag^{C938A} (200 pg RNA). (*E–H*) Immunoblot analysis of pSmad2 levels in st. 11 Tril or Con morphants expressing wild-type Nedd4lFlag (*E* and *F*) or constitutively active Nedd4l^{R893Q} (200 pg RNA) (*G* and *H*) in dorsal cells. (*I* and *J*) In vitro autoubiquitination assay performed on Nedd4lFlag IP from Con or Tril morphants. (*K*) Nedd4l ubiquitinates and targets Nodal receptors for degradation in a Smad7 dependent manner to reduce pathway activation while Smurf plays an analogous role in dampening Bmp signaling. Tril triggers degradation of Smad7 and simultaneously activates Nedd4l. (*L*) In Tril morphants, elevated levels of Smad7 recruit Nedd4l to Nodal receptors, and Smurf to Bmp receptors, but Nedd4l is less active. BMP signaling is depressed while Nodal output is elevated in Tril morphants.

(Fig. 4 *G* and *H*). The ability of constitutively active but not wild-type Nedd4l to reduce pSmad2 levels in Tril morphants demonstrates that Tril does not dampen Nodal activity merely by enhancing Nedd4l protein levels.

To ask whether Tril is required for enzymatic activation of Nedd4l, we expressed wild-type or catalytically dead (Nedd4l-Flag^{C938A}) Nedd4l together with control or Tril MOs in embryos. Nedd4lFlag was immunoprecipitated (IP) from embryos at stage 11 and subjected to an in vitro autoubiquitination assay using recombinant E1, E2, ATP, and HA-ubiquitin. Wild-type Nedd4l exhibited high levels of ubiquitination in control morphants, while Nedd4l^{C938A} was not ubiquitinated, confirming that ubiquitination of wild-type Nedd4l was autocatalytic. In Tril morphants, autoubiquitination was reduced to 12 to 38% of control (when normalized to Nedd4lFlag levels) (Fig. 4 *I* and *J*). Thus, Tril dampens Nodal pathway output by triggering enzymatic activation of Nedd4l.

Our data, along with previously published findings, support the following hypothetical working model that accounts for the paradoxical finding that Tril dampens Nodal signaling despite triggering degradation of the Nodal inhibitor, Smad7. In wild-type embryos, Nedd4l ubiquitinates and targets Nodal receptors for degradation in a Smad7-dependent manner to reduce pathway activation (19) (Fig. 4*K*). A distinct HECT family E3 ligase, most likely Smurf1 (24), plays an analogous role in dampening Bmp signaling. Tril uncouples the effects of Smad7 on the Bmp and Nodal pathways by simultaneously triggering degradation of Smad7 and activating Nedd4l (Fig. 4*K*). In wild-type embryos, we propose that Nedd4l and Smurf1 compete for binding to the endogenous pool of Smad7 to maintain a proper balance of Nodal and Bmp signaling. In Tril morphants, elevated levels of Smad7 recruit Nedd4l and Smurf to Nodal and Bmp receptors, respectively, but Nedd4l is less active, resulting in down-regulation of ubiquitination of Nodal receptors (Fig. 4*L*). This tips the balance toward Smad7/Smurf1-mediated degradation of Bmp receptors and lessens degradation of Nodal receptors to enhance Nodal signaling (Fig. 4*L*).

Peli2 Binds to the Cytoplasmic Tail of Tril and Dampens Nodal Signaling by Activating Nedd4l. To identify Tril-interacting proteins that might transduce downstream signals to activate Nedd4l, we performed a yeast two-hybrid screen with the Tril ICD as bait and a *Xenopus* gastrula stage complementary DNA (cDNA) library as prey. We identified Pellino E3 ubiquitin ligase family member 2 (Peli2) as a Tril binding partner. Peli2 is one of three members of an E3 ligase family that binds phosphorylated substrates via an amino terminal forkhead-associated (FHA) domain and catalyzes Lys63-linked ubiquitination of substrates via a RING domain (25) (Fig. 5*A*). Peli2-HA and Tril-Flag were coexpressed in *Xenopus* embryos, and Tril was IP using antibodies specific for Flag. Proteins in immunoprecipitates or in lysates (input) were separated by sodium dodecyl sulfate polyacrylamide gel electrophoresis (SDS-PAGE), and immunoblots were probed with antibodies specific for HA or for Flag. As shown in Fig. 5*B*, Peli2 co-IP with full length Tril. Furthermore, Peli2 co-IP with a deletion mutant form of Tril (TrilΔECD) lacking the ECD when the two were coexpressed in HEK293T cells (*SI Appendix,* Fig. S4*A*). Finally, when antibodies that recognize Peli1 and Peli2 were used to pull down Peli1/2 from HEK293T or HeLa cells, and immunoblots were probed with antibodies specific for Tril, the endogenous proteins co-IP (Fig. 5*C*).

Peli2 transcripts were present maternally and persisted throughout development (Fig. 5*D*). *Peli2* transcripts were ubiquitously distributed in cleavage (Fig. 5*E*) through late blastula stage embryos (Fig. 5*F*) but became enriched in dorsal mesoderm by the onset of gastrulation (Fig. 5*G*, arrows). By midgastrulation, *peli2* transcripts were concentrated in a thin stripe distal to the dorsal blastopore (Fig. 5*H*) and by late gastrulation were expressed

in the dorsolateral mesoderm and excluded from a stripe of cells at the dorsal midline (Fig. 5*I*, arrow). Thus, *peli2* is expressed at the right time and place to function downstream of Tril.

We generated two antisense MOs that target the 5′ untranslated region of both *Xenopus peli2* homeologs and verified that these blocked translation of *peli2* messenger RNAs (mRNAs) (*SI Appendix,* Fig. S4*B*). Depletion of Peli2 in dorsal cells, using either of the two MOs, phenocopied the defects in axial extension and head development observed in Tril morphants (Fig. 5 *J* and *K* and *SI Appendix,* Fig. S4 *C* and *D*). Furthermore, expression of *nodal1* and *nodal2* was elevated in Peli2 morphants (Fig. 5*L*). Levels of pSmad2 were also elevated in Peli2 morphants (Fig. 5 *M* and *N*), and these were rescued by coinjection of Peli2 RNA lacking the MO target sequence (*SI Appendix,* Fig. S4*E*). Thus, Peli2 is required to dampen Nodal signaling to allow for normal gastrulation and head development.

We used in vitro ubiquitination assays to compare levels of Nedd4l activation in control and Peli2 morphant embryos. In Peli2 morphants, autoubiquitination of Nedd4l was reduced to 25 to 60% of control (when normalized to Nedd4lFlag levels) (Fig. 5 *O* and *P*). In addition, steady-state levels of endogenous Nedd4l were reduced in Peli2 morphants (*SI Appendix,* Fig. S4 *F* and *G*). Thus, Peli2, like Tril, is required to stabilize and to enzymatically activate Nedd4l.

We then coexpressed Peli2 and Nedd4l in *Xenopus* embryos, IP Nedd4l, and probed immunoblots with antibodies that recognized Peli2HA. Peli2 co-IP with Nedd4l (Fig. 5*Q*), indicating that the two proteins form a complex in vivo.

Catalytic activation of Nedd4l requires JNK-mediated phosphorylation of threonine 899 (T899) (26). Phosphorylation of Nedd4l^{T899} creates a phospho-motif (pTXXS) that is recognized as a substrate-binding site by the FHA domain of Peli2 (27). We coexpressed Peli2HA together with Nedd4l-Flag^{T899A} in *Xenopus* embryos and repeated coimmunoprecipitation assays. Peli2 efficiently co-IP with Nedd4l^{T899A} (*SI Appendix,* Fig. S4*H*), indicating that phosphorylation of Nedd4l^{T899} is not required for interaction with Peli2.

We then performed coimmunoprecipitation assays on embryos expressing Nedd4lFlag together with a form of Peli2 that does not recognize phosphthreonine motifs (Peli2^{R104A}) or with a catalytically inactive mutant (Peli2^{H315A}). Relative to wild-type Peli2, very little Peli2^{R104A} co-IP with Nedd4l (*SI Appendix,* Fig. S4*I*). Thus, the ability of Peli2 to bind phosphothreonine motifs, either on Nedd4l itself (other than T899) or on another interacting protein, is essential for efficient interaction with Nedd4l in vivo. By contrast, much higher levels of Peli2^{H315A} co-IP with Nedd4l relative to wild-type Peli2 in both *Xenopus* embryos (*SI Appendix,* Fig. S4*I*) and in HEK293T cells (*SI Appendix,* Fig. S4*J*), suggesting that the catalytic activity of Peli2 is required for its release from Nedd4l.

To ask whether Peli2 is sufficient to activate Nedd4l, we coexpressed Nedd4lFlag and ubiquitin-HA in HEK293T cells in the presence or absence of Peli2 or Peli2^{H315A}. Nedd4lFlag was IP from cells, and immunoblots were probed for ubiquitin-HA. Peli2 induced a twofold increase in ubiquitination of Nedd4l but not Nedd4l^{C938A} (Fig. 5 *R* and *S*). A dramatic increase in ubiquitination of both Nedd4l and Nedd4l^{C938A} was observed when either was coexpressed with catalytically inactive Peli2^{H315A} (Fig. 5*R*). Collectively, our data show that Peli2 is both necessary and sufficient to activate the catalytic activity of Nedd4l, without directly ubiquitinating it. Furthermore, Peli2^{H315A}, which is not readily released from Nedd4l, recruits an independent ubiquitin ligase to the complex that can directly ubiquitinate Nedd4l.

Traf6 Is Required for Membrane Recruitment and Catalytic Activation of Nedd4l. Peli1 and Peli2 collaborate with TNF-receptor associated factor 6 (Traf6) to ubiquitinate substrates in the TLR signaling pathway (28), raising the possibility that Traf6 is the
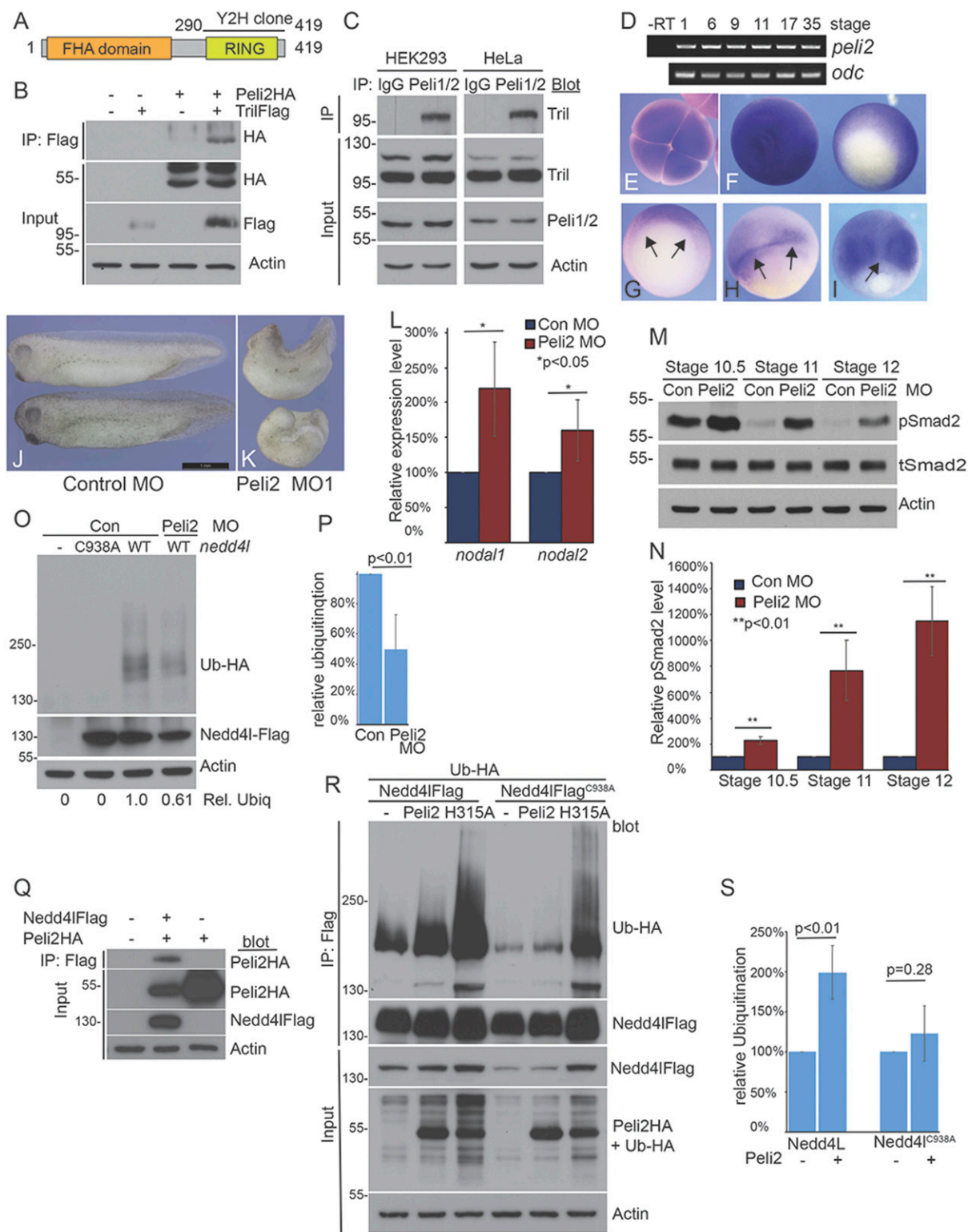
Kim et al.
Tril dampens Nodal signaling through Pellino2- and Traf6-mediated activation of Nedd4l

PNAS | 7 of 12
https://doi.org/10.1073/pnas.2104661118

Fig. 5. Peli2 binds to the cytoplasmic tail of Tril and dampens Nodal signaling by activating Nedd4l. (*A*) Illustration of Peli2 structure. (*B*) Peli2HA and TrilFlag were coexpressed in *Xenopus* embryos, and Tril was IP from st. 11 embryo lysates. Immunoblots of IPs or cell lysates (input) were probed with antibodies that recognize HA or Flag. (*C*) HEK293 or HeLa cell lysates were subject to IP with antibodies that recognize Peli1 and Peli2 or control (Con) IgG. Immunoblots of IPs were probed with antibodies that recognize Tril. (*D–I*) RT-PCR analysis (*D*) or whole mount in situ hybridization analysis of *peli2* expression at st. 3 (*E*), 9 (*F*), 10 (*G*), 11 (*H*), and 12 (*I*). Arrows: dorsal blastopore. (*J* and *K*) Con or Peli2 MO1 (15 ng) was injected into dorsal cells of four-cell embryos. Representative embryos were photographed at st. 34. (Scale bar: 1 mm.) (*L–N*) Expression of *nodal1* and *nodal2* was analyzed by qPCR (*L*) or pSmad2 levels were analyzed by immunoblot (*M* and *N*) in Peli2 or Con morphants. (*O* and *P*) Nedd4lFlag was IP from Con or Peli2 morphants at st. 11 and subjected to an in vitro autoubiquitination assay. (*Q*) Nedd4lFlag and Peli2HA were coexpressed in *Xenopus* embryos. Nedd4l was IP from embryo lysates at st. 11. Immunoblots of IPs were probed for HA. (*R* and *S*) Nedd4lFlag or Nedd4lFlag^{C938A} was coexpressed with ubiquitin-HA (Ub-HA) in HEK293 cells in the presence or absence of Peli2 or Peli2^{H315A}. Nedd4l was IP from cells using antibodies that recognize the Flag tag, and immunoblots of IPs were probed for Ub-HA.

ubiquitin ligase recruited to the Peli2^{H315A}/Nedd4l complex. To test this, we performed coimmunoprecipitation assays in HEK293T cells expressing Nedd4lFlag alone or together with Peli2HA and/or Traf6Myc. Traf6 co-IP with Nedd4l in the presence, and in the absence, of wild-type or catalytically inactive Peli2 (Fig. 6A).

We next asked whether Traf6 is sufficient to activate Nedd4l. Nedd4lFlag was coexpressed with ubiquitin-HA in HEK293T cells in the presence or absence of Traf6 and/or Peli2. Whereas Peli2 induced a twofold increase in ubiquitination of Nedd4l (Fig. 6B, lane 3) but not Nedd4l^{C938A} (lane 7), Traf6 induced a much higher level of ubiquitination of Nedd4l in the presence and absence of Peli2 (Fig. 6B, lanes 2 and 4) and ubiquitinated catalytically inactive Nedd4l^{C938A} in the absence of Peli2 (Fig. 6B, lane 6). Thus, Traf6, like Peli2, is sufficient to trigger the catalytic activity of Nedd4l, and Traf6 can ubiquitinate Nedd4l.

We then coexpressed Nedd4lFlag with ubiquitin-HA in HEK293T cells in the presence or absence of Peli2 alone or together with a dominant mutant form of Traf6 (Traf6C) (29). Peli2 induced a robust increase in ubiquitination of Nedd4l that was abolished in the presence of Traf6C (Fig. 6 C and D) showing that Traf6 is required for Peli2-mediated activation of Nedd4l in mammalian cells.

To ask whether Traf6 is required for activation of Nedd4l in *Xenopus*, we expressed Nedd4lFlag alone or together with Traf6C and performed in vitro autoubiquitination assays. Autoubiquitination of Nedd4l was reduced to 50% of control in the presence of Traf6C (Fig. 6 E and F). Notably, *traf6* transcripts are ubiquitously expressed in *Xenopus* gastrula and appear to be more abundant in dorsal and lateral cells than in ventral cells (*SI Appendix*, Fig. S5 A–C).

How might Peli2/Traf6 trigger the catalytic activity of Nedd4l? Nedd4l normally exists in a closed, inactive conformation (22). Src-mediated phosphorylation of Nedd4l on a key Tyrosine residue triggers a conformational switch that relieves autoinhibition (30), and Traf6 can recruit and activate c-Src (31–33). To test the possibility that Traf6 triggers Src-mediated activation of Nedd4l in *Xenopus*, we used in vitro ubiquitination assays to compare activation in the presence and absence of the Src inhibitor, C-terminal Src Kinase (CSK). CSK did not impair activation of Nedd4l (*SI Appendix*, Fig. S5D, lanes 3 versus 4). Furthermore, although a form of Nedd4l (Nedd4l^{Y481E}) shown to mimic the phosphorylation event that relieves autoinhibition is hyperactivated in *Xenopus* (*SI Appendix*, Fig. S5D, lane 3 versus 6), mutation of the same tyrosine to a nonphosphorylatable residue (Nedd4l^{Y481F}) does not impair activation (*SI Appendix*, Fig. S5D, lanes 3 versus 5). Thus, Peli2/Traf6-mediated activation of Nedd4l does not appear to involve phosphorylation on Y481.

Another way that Traf6 might trigger the catalytic activity of Nedd4l is by promoting its translocation to cellular membranes (22, 23). We expressed Nedd4lFlag alone or together with Traf6C HA in *Xenopus* embryos, isolated ectodermal explants at the gastrula stage, and immunostained them for Flag and HA. When Nedd4l was expressed alone, it localized to the plasma membrane, intracellular puncta, and vesicular appearing structures (Fig. 6G, arrows). By contrast, when coexpressed with Traf6C, Nedd4l was retained in the cytoplasm surrounding the embryonic yolk platelets in a pattern coincident with that of Traf6C.

Our studies support the following working model for how Tril activates Nedd4l to dampen Nodal signaling (Fig. 6H). We have previously shown that Tril must be internalized to signal in *Xenopus* (14) and propose that the Tril-interacting protein, Peli2, is internalized along with Tril (1). It is possible that Tril is internalized along with Tlr3/4 in response to an endogenous ligand (*Discussion*). Peli2 then binds to Nedd4l together with Traf6 (2), and Traf6 ubiquitinates Nedd4l to allow for membrane translocation and activation (3). Nedd4l is then recruited to the activated Nodal receptor by Smad7 (4) and triggers its degradation (5).

Discussion

The current studies identify a signal transduction cascade that functions downstream of Tril to coordinately enhance BMP signaling and dampen Nodal signaling. We show that Tril tips the balance of Smad7-mediated inhibition to favor Nodal, rather than BMP inhibition. It does so by simultaneously stimulating Smad7 degradation (5) and activating Nedd4l. Finally, we show that Peli2 and Traf6, which transduce Tril/Tlr signaling during innate immunity in adults, are also used to transduce Tril signals in a developmental context.

Nedd4l is a multifaceted ubiquitin ligase that regulates diverse signal transduction pathways. In addition to targeting Nodal pathway components, Nedd4l targets the Wnt pathway proteins LGR5 (34) and Dvl (20, 35) to negatively regulate canonical and noncanonical Wnt signaling. When Nedd4l activity is reduced, Dvl protein levels are elevated (20), and this leads to gastrulation defects (36, 37). Additional Nedd4l substrates include the Epithelial Sodium Channel, AKT/mTor pathway components, and proteins required for mast cell activation, autophagy, multivesicular body formation, and viral shedding, among others (38). Mutations or single nucleotide polymorphisms in the human *NEDD4L* gene are associated with asthma, hypertension, end-stage renal disease, periventricular nodular heterotopia, and idiopathic epilepsy (38), underscoring the importance of this gene to human pathology. Understanding how Nedd4l activity is regulated in different contexts may shed light on how these mutations cause disease and congenital defects in humans.

Nedd4 family members contain a C2 domain followed by several WW substrate-binding modules and a HECT (homologous to E6-AP carboxyl terminus) catalytic domain. Nedd4 E3 ligases exist in an inactive form at steady state. In the case of NEDD4L, structural studies have revealed that the C2 domain binds calcium using the same interface that interacts with the HECT domain (22). It has been proposed that elevated calcium causes NEDD4L to translocate to the membrane, where calcium binds to the C2 domain and disrupts interactions with the HECT domain, causing a transition to the open, active state (22, 39). There is also evidence that unidentified membrane proteins function independent of calcium to facilitate this transition (39). In other contexts, c-Src phosphorylates a critical Tyrosine residue between two WW domains to induce a shift to an active conformation. In the current studies, we identify players in Nedd4l activation in the context of vertebrate development and in mammalian cells. We show that Tril, the Tril-interacting protein Peli2, and its binding partner Traf6 are all required for activation of Nedd4l and that Traf6 can ubiquitinate Nedd4l and is required for recruitment of Nedd4l to membrane compartments. Further studies will be required to determine whether Traf6-mediated ubiquitination of Nedd4l is necessary and/or sufficient for membrane translocation and activation or whether this requires Traf6-mediated mobilization of intracellular calcium or activation of other signaling pathways.

Our findings reveal that Peli2 and Traf6 are both required to activate Nedd4l, but the individual role of these ubiquitin ligases is unclear. Peli2 and Traf6 interact with each other (28), raising the possibility that one recruits the other to the Nedd4l complex. This seems unlikely, however, given that coexpression of Peli2 and Traf6 does not enhance recruitment of either protein to the Nedd4l complex. Another possibility is that Peli2 provides a scaffold for dimerization, autoubiquitination, and activation of Traf6. Notably, the catalytic activity of Peli2 is required for its release from the Nedd4l complex suggesting that binding and ubiquitination is a dynamic process in which Peli2 transiently interacts with Nedd4l and is then rapidly released, allowing Traf6 to function. Future studies will elucidate the specific function of each of these proteins in activation of Nedd4l, both in *Xenopus* and in mammalian cells.
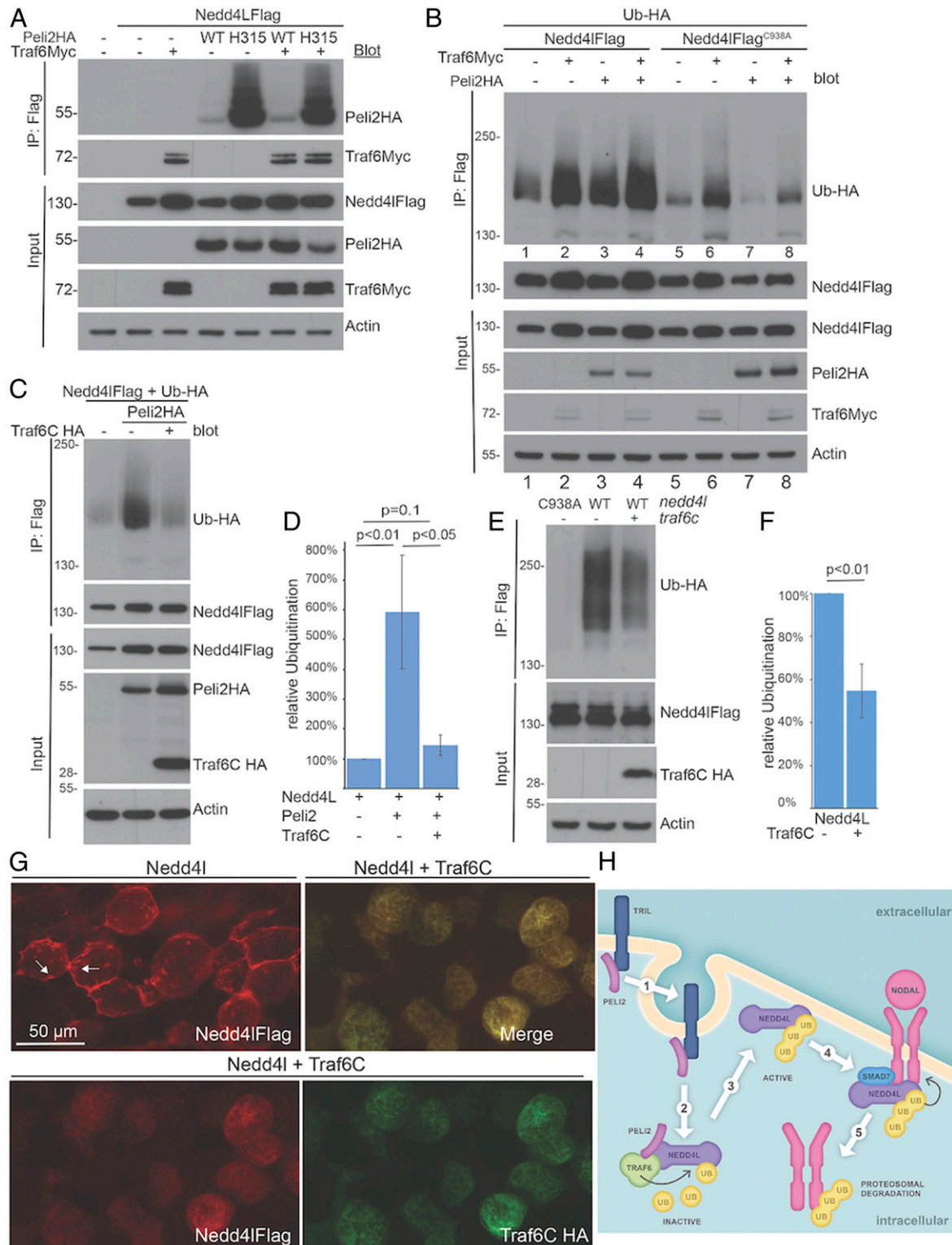
Kim et al.
Tril dampens Nodal signaling through Pellino2- and Traf6-mediated activation of Nedd4l

PNAS | 9 of 12
https://doi.org/10.1073/pnas.2104661118

Fig. 6. Traf6 is required for membrane recruitment and catalytic activation of Nedd4l. (*A*) Nedd4lFlag was coexpressed in HEK 293T cells $^{+/-}$ wild-type Peli2HA, Peli2HA^{H315A}, and/or Traf6Myc. Nedd4l was IP from cells, and immunoblots of IPs were probed for Traf6Myc. (*B–D*) Nedd4l or Nedd4lFlag^{C938A} was coexpressed with ubiquitin-HA (Ub-HA) in HEK293T cells $^{+/-}$ Peli2HA and/or Traf6Myc (*B*) or together with Traf6C (*C* and *D*). Nedd4l was IP from cells, and immunoblots of IPs were probed for Ub-HA. (*E* and *F*) Nedd4lFlag was expressed alone or together with Traf6C in embryos, IP at st. 11, and subjected to an in vitro autoubiquitination assay. (*G*) Immunostaining of ectodermal explants isolated from gastrula stage embryos expressing Nedd4lFlag alone or together with Traf6C HA. White arrows denote intracellular vesicular structures. (Scale bar: 50 μM.) (*H*) The Tril-interacting protein, Peli2, is internalized along with Tril (1), binds to Nedd4l together with Traf6 (2), and both are required for membrane translocation and activation of Nedd4l (3). Activated Nedd4l is recruited to the Nodal receptor by Smad7 (4), and ubiquitinates it, targeting it for proteosomal degradation (5). Image credit: Anne Martin (artist).

Another unanswered question is whether Tril functions independent of Tlr3/4 to stimulate activation of Nedd4l or whether it serves as a coreceptor for Tlrs in the context of early development. Tlrs bind microbial products or nucleic acids, initiating a signaling cascade involving cytoplasmic adaptors and kinases that function upstream of Traf6 and Peli, and generally culminates in activation of transcriptional regulators such as NF-κB (40). While Tlrs are known to play nonimmune roles in developmental patterning and morphogenesis in insects, there is currently no evidence that these roles are conserved during vertebrate development (41). Recent studies, however, have identified roles for Tlrs within the brain of mammals, although little is known about the ligands and signaling pathways that mediate these nonimmune effects (42). Our findings raise the intriguing possibility that Tlr/Tril signaling activates a noncanonical, NF-κB independent signaling cascade during early vertebrate development.

In the context of innate immunity, the ECD of Tril interacts directly with Tlr4 and with its ligand lipopolysaccharide, suggesting that it functions primarily to enhance ligand–receptor affinity (6). By contrast, our structure–function analysis shows that Tril cycles between the cell surface and endosomes in embryos and that the ICD of Tril is indispensable for downstream signaling, most likely because it is required for internalization of Tril (14) and also for recruitment of Peli2 (current studies). These studies also show that the Tril ECD and cadherin based cell–cell adhesion are required for its cell-surface retention. A deletion mutant lacking the ECD is constitutively internalized and signaling incompetent (14). This suggests that Tril is tethered at the plasma membrane through interactions with additional membrane proteins until signaling is initiated, consistent with a model in which Tril binds to Tlr3 or 4 and is internalized together with these receptors following activation by endogenous ligands. Further studies will be required to document the upstream events that initiate signaling downstream of Tril during embryonic development.

Materials and Methods

***Xenopus* Embryo Culture and Manipulation.** Animal procedures followed protocols approved by the University of Utah Institutional Animal Care and Use Committee. Embryos were obtained, microinjected, and cultured as described (43). Embryo explants were performed as described (44). Embryos were stained for β-galactosidase activity using Red-Gal (Sigma) and processed for in situ hybridization as described (45) except that the vitelline coat was not removed prior to fixation, and BM purple (Roche) was used as a substrate.

Morpholinos and cDNA Constructs. Tril MOs (5), Nedd4l MOs (20), and Peli2 MOs (MO1 5′-AAAACATGGAGAAGACGGTCCCCGT-3′; MO2 5′-CATGGCAGC-TCATATACACACCGGA-3′) were purchased from Gene Tools. Nedd4lFlag and Nedd4lFlag^{C938A} were obtained from Dr. Quinghua Tao (Tsinghua University, Beijing), and Nedd4lFlag^{T899A} was obtained from Dr. Vivek Bhalla (Stanford University). Other point mutant forms of Nedd4lFlag, Peli2HA, and ca-Smad2 were generated using a QuikChange II XL site-directed mutagenesis kit (Agilent Technologies). Traf6Myc, Traf6C, and Peli2HA were generated using PCR-based methods.

Immunostaining. Explants were fixed and immunostained as described (5) using antibodies listed in *SI Appendix*, Table S2.

Yeast Two-Hybrid Screening. Sequence encoding the Tril ICD was ligated into the vector pGBKT7 to create an in-frame fusion with the GAL4 DNA-binding domain, and this bait plasmid was transformed into yeast strain PJ69-4A. A pGAD10 *Xenopus* gastrula stage cDNA library (46) was then transformed into the bait containing yeast strain. Two-hybrid screening was performed according to the manufacturer's instruction (Clontech, MatchMaker System 3). Positive clones showing colony formation in minimal growth medium lacking tryptophan, leucine, and adenine were selected. Recovered plasmids were identified by DNA sequencing.

Analysis of RNA. Total RNA was isolated using TRIzol (Invitrogen). qPCR (44) and semi qRT-PCR (47) were performed as described using an annealing temperature of 58 °C and primers listed in *SI Appendix*, Table S1.

Transient Transfection and Immunoprecipitation. HEK293T and HeLa cells were maintained at 37 °C in a humidified incubator containing 5% CO_2 and were mycoplasm free. Cells were plated on 10-cm culture plates and transiently transfected with a total of 3 μg plasmid DNA or empty vector using Lipofectamine 2000 (Invitrogen). Cells were cultured for 48 h before harvesting for immunoblots or IP. Harvested cells were homogenized in IP lysis buffer (150 mM NaCl, 20 mM Tris-Cl pH 7.5, 1 mM EDTA, 1% Sodium deoxycholate, 1% Nonidet P-40, 1× protease/phosphatase inhibitor). *Xenopus* embryos were homogenized in 20 μL IP lysis buffer (150 mM NaCl, 50 mM Tris-Cl pH 7.5, 1 mM EDTA, 1% TritonX-100, 1× protease/phosphatase inhibitor) per embryo equivalent. A total of 500 μg cell lysate or 1,000 μL *Xenopus* extract from 30 embryos were used for coimmunoprecipitation assays as described (48) using the primary antibodies listed in *SI Appendix*, Table S2. Proteins were diluted in 40 μL 2× Laemmli sample buffer and boiled for 5 min prior to SDS-PAGE and immunoblot analysis.

In Vitro Ubiquitination Assay. Nedd4lFlag and Nedd4lFlag^{C938A} were IP from *Xenopus* embryos and diluted in 40 μl ubiquitination reaction buffer (20 mM Hepes pH 7.2, 100 mM NaCl). Nedd4l-directed autoubiquitination assays were carried out in 45 μL reactions containing 30 μL IP Nedd4lFlag, 10 μM Ub-HA (R&D Systems), 0.1 μM E1 (UBA1, Boston Biochem), 0.2 μM E2 (UBE2L3, Boston Biochem), and 1× proteinase inhibitor (Thermo). Reactions were incubated for 1 h at 37 °C after addition of 5 mM ATP-10 mM $MgCl_2$. After addition of one-third volume of 4× Laemmli sample buffer, reaction products were boiled for 5 min prior to immunoblot analysis.

Immunoblots. Embryos were lysed in Triton X-100 lysis buffer (49), and HEK293 or HeLa cells were lysed in IP buffer containing HALT protease inhibitor and phosphatase mixture (Thermo Scientific). Immunoblots were performed as described (50) using primary antibodies listed in *SI Appendix*, Table S2.

Statistics. NIH Image J software was used to quantify band intensities. A Student's *t* test was used to compare differences in gene expression or protein levels between two groups. Differences with $P < 0.05$ were considered statistically significant. Unless stated otherwise, all results were reproduced in three biological replicates, and quantitative experiments were averaged with SD reported.

Data Availability. All study data are included in the article and/or *SI Appendix*.

1. J. Heasman, Patterning the early *Xenopus* embryo. *Development* **133**, 1205–1217 (2006).
2. B. Thisse, C. Thisse, Formation of the vertebrate embryo: Moving beyond the Spemann organizer. *Semin. Cell Dev. Biol.* **42**, 94–102 (2015).
3. L. M. Wakefield, C. S. Hill, Beyond TGFβ: Roles of other TGFβ superfamily members in cancer. *Nat. Rev. Cancer* **13**, 328–341 (2013).
4. X. Yan, Y. G. Chen, Smad7: Not only a regulator, but also a cross-talk mediator of TGF-β signalling. *Biochem. J.* **434**, 1–10 (2011).
5. Y. S. Green, S. Kwon, M. S. Mimoto, Y. Xie, J. L. Christian, Tril targets Smad7 for degradation to allow hematopoietic specification in *Xenopus* embryos. *Development* **143**, 4016–4026 (2016).
6. S. Carpenter *et al.*, TRIL, a functional component of the TLR4 signaling complex, highly expressed in brain. *J. Immunol.* **183**, 3989–3995 (2009).
7. S. Carpenter, P. Wochal, A. Dunne, L. A. J. O'Neill, Toll-like receptor 3 (TLR3) signaling requires TLR4 Interactor with leucine-rich REPeats (TRIL). *J. Biol. Chem.* **286**, 38795–38804 (2011).
8. P. Wochal *et al.*, TRIL is involved in cytokine production in the brain following *Escherichia coli* infection. *J. Immunol.* **193**, 1911–1919 (2014).
9. C. M. Jones, M. R. Kuehn, B. L. Hogan, J. C. Smith, C. V. Wright, Nodal-related signals induce axial mesoderm and dorsalize mesoderm during gastrulation. *Development* **121**, 3651–3662 (1995).
10. E. M. Joseph, D. A. Melton, Xnr4: A *Xenopus* nodal-related gene expressed in the Spemann organizer. *Dev. Biol.* **184**, 367–372 (1997).

Kim et al.
Tril dampens Nodal signaling through Pellino2- and Traf6-mediated activation of Nedd4l

PNAS | 11 of 12
https://doi.org/10.1073/pnas.2104661118

DEVELOPMENTAL BIOLOGY

11. S. Takahashi *et al*., Nodal-related gene Xnr5 is amplified in the *Xenopus* genome. *Genesis* **44**, 309–321 (2006).

12. S. Takahashi *et al*., Two novel nodal-related genes initiate early inductive events in *Xenopus* Nieuwkoop center. *Development* **127**, 5319–5329 (2000).

13. Y. S. Lee *et al*., Smad7 and Smad6 bind to discrete regions of Pellino-1 via their MH2 domains to mediate TGF-beta1-induced negative regulation of IL-1R/TLR signaling. *Biochem. Biophys. Res. Commun.* **393**, 836–843 (2010).

14. H. S. Kim, A. McKnite, Y. Xie, J. L. Christian, Fibronectin type III and intracellular domains of Toll-like receptor 4 interactor with leucine-rich repeats (Tril) are required for developmental signaling. *Mol. Biol. Cell* **29**, 523–531 (2018).

15. J. Yao, D. S. Kessler, Goosecoid promotes head organizer activity by direct repression of Xwnt8 in Spemann's organizer. *Development* **128**, 2975–2987 (2001).

16. M. Artinger, I. Blitz, K. Inoue, U. Tran, K. W. Cho, Interaction of goosecoid and brachyury in *Xenopus* mesoderm patterning. *Mech. Dev.* **65**, 187–196 (1997).

17. W. W. Branford, H. J. Yost, Lefty-dependent inhibition of Nodal- and Wnt-responsive organizer gene expression is essential for normal gastrulation. *Curr. Biol.* **12**, 2136–2141 (2002).

18. E. Reissmann *et al*., The orphan receptor ALK7 and the Activin receptor ALK4 mediate signaling by Nodal proteins during vertebrate development. *Genes Dev.* **15**, 2010–2022 (2001).

19. G. Kuratomi *et al*., NEDD4-2 (neural precursor cell expressed, developmentally down-regulated 4-2) negatively regulates TGF-beta (transforming growth factor-beta) signalling by inducing ubiquitin-mediated degradation of Smad2 and TGF-beta type I receptor. *Biochem. J.* **386**, 461–470 (2005).

20. Y. Zhang, Y. Ding, Y. G. Chen, Q. Tao, NEDD4L regulates convergent extension movements in *Xenopus* embryos via Disheveled-mediated non-canonical Wnt signaling. *Dev. Biol.* **392**, 15–25 (2014).

21. S. Gao *et al*., Ubiquitin ligase Nedd4L targets activated Smad2/3 to limit TGF-beta signaling. *Mol. Cell* **36**, 457–468 (2009).

22. A. Escobedo *et al*., Structural basis of the activation and degradation mechanisms of the E3 ubiquitin ligase Nedd4L. *Structure* **22**, 1446–1457 (2014).

23. L. Broix *et al*.; Deciphering Developmental Disorders study, Mutations in the HECT domain of NEDD4L lead to AKT-mTOR pathway deregulation and cause periventricular nodular heterotopia. *Nat. Genet.* **48**, 1349–1358 (2016).

24. H. Zhu, P. Kavsak, S. Abdollah, J. L. Wrana, G. H. Thomsen, A SMAD ubiquitin ligase targets the BMP pathway and affects embryonic pattern formation. *Nature* **400**, 687–693 (1999).

25. F. Humphries, P. N. Moynagh, Molecular and physiological roles of Pellino E3 ubiquitin ligases in immunity. *Immunol. Rev.* **266**, 93–108 (2015).

26. K. R. Hallows *et al*., Phosphopeptide screen uncovers novel phosphorylation sites of Nedd4-2 that potentiate its inhibition of the epithelial Na+ channel. *J. Biol. Chem.* **285**, 21671–21678 (2010).

27. Y. S. Huoh, K. M. Ferguson, The Pellino E3 ubiquitin ligases recognize specific phosphothreonine motifs and have distinct substrate specificities. *Biochemistry* **53**, 4946–4955 (2014).

28. S. Strickson *et al*., Roles of the TRAF6 and Pellino E3 ligases in MyD88 and RANKL signaling. *Proc. Natl. Acad. Sci. U.S.A.* **114**, E3481–E3489 (2017).

29. Z. Cao, J. Xiong, M. Takeuchi, T. Kurama, D. V. Goeddel, TRAF6 is a signal transducer for interleukin-1. *Nature* **383**, 443–446 (1996).

30. N. J. Grimsey *et al*., A tyrosine switch on NEDD4-2 E3 ligase transmits GPCR inflammatory signaling. *Cell Rep.* **24**, 3312–3323.e5 (2018).

31. A. Liu *et al*., TRAF6 protein couples Toll-like receptor 4 signaling to Src family kinase activation and opening of paracellular pathway in human lung microvascular endothelia. *J. Biol. Chem.* **287**, 16132–16145 (2012).

32. K. Z. Wang *et al*., TRAF6 activation of PI 3-kinase-dependent cytoskeletal changes is cooperative with Ras and is mediated by an interaction with cytoplasmic Src. *J. Cell Sci.* **119**, 1579–1591 (2006).

33. B. R. Wong *et al*., TRANCE, a TNF family member, activates Akt/PKB through a signaling complex involving TRAF6 and c-Src. *Mol. Cell* **4**, 1041–1049 (1999).

34. L. Novellasdemunt *et al*., NEDD4 and NEDD4L regulate Wnt signalling and intestinal stem cell priming by degrading LGR5 receptor. *EMBO J.* **39**, e102771 (2020).

35. Y. Ding, Y. Zhang, C. Xu, Q. H. Tao, Y. G. Chen, HECT domain-containing E3 ubiquitin ligase NEDD4L negatively regulates Wnt signaling by targeting Dishevelled for proteasomal degradation. *J. Biol. Chem.* **288**, 8289–8298 (2013).

36. S. Y. Sokol, Analysis of Dishevelled signalling pathways during *Xenopus* development. *Curr. Biol.* **6**, 1456–1467 (1996).

37. J. B. Wallingford *et al*., Dishevelled controls cell polarity during *Xenopus* gastrulation. *Nature* **405**, 81–85 (2000).

38. J. A. Manning, S. Kumar, Physiological functions of Nedd4-2: Lessons from knockout mouse models. *Trends Biochem. Sci.* **43**, 635–647 (2018).

39. J. Wang *et al*., Calcium activates Nedd4 E3 ubiquitin ligases by releasing the C2 domain-mediated auto-inhibition. *J. Biol. Chem.* **285**, 12279–12288 (2010).

40. S. W. Brubaker, K. S. Bonham, I. Zanoni, J. C. Kagan, Innate immune pattern recognition: A cell biological perspective. *Annu. Rev. Immunol.* **33**, 257–290 (2015).

41. F. Leulier, B. Lemaitre, Toll-like receptors—Taking an evolutionary approach. *Nat. Rev. Genet.* **9**, 165–178 (2008).

42. N. Anthoney, I. Foldi, A. Hidalgo, Toll and Toll-like receptor signalling in development. *Development* **145**, dev156018 (2018).

43. M. S. Mimoto, J. L. Christian, Manipulation of gene function in *Xenopus laevis*. *Methods Mol. Biol.* **770**, 55–75 (2011).

44. M. S. Mimoto, S. Kwon, Y. S. Green, D. Goldman, J. L. Christian, GATA2 regulates Wnt signaling to promote primitive red blood cell fate. *Dev. Biol.* **407**, 1–11 (2015).

45. R. M. Harland, In situ hybridization: An improved whole-mount method for *Xenopus* embryos. *Methods Cell Biol.* **36**, 685–695 (1991).

46. A. D. Agulnick *et al*., Interactions of the LIM-domain-binding factor Ldb1 with LIM homeodomain proteins. *Nature* **384**, 270–272 (1996).

47. T. Nakayama *et al*., *Xenopus* Smad8 acts downstream of BMP-4 to modulate its activity during vertebrate embryonic patterning. *Development* **125**, 857–867 (1998).

48. H.-S. Kim, J. Neugebauer, A. McKnite, A. Tilak, J. L. Christian, BMP7 functions predominantly as a heterodimer with BMP2 or BMP4 during mammalian embryogenesis. *Elife* **8**, e48872 (2019).

49. S. C. Choi, J. K. Han, Rap2 is required for Wnt/beta-catenin signaling pathway in *Xenopus* early development. *EMBO J.* **24**, 985–996 (2005).

50. S. Kwon, J. L. Christian, Sortilin associates with transforming growth factor-beta family proteins to enhance lysosome-mediated degradation. *J. Biol. Chem.* **286**, 21876–21885 (2011).